

## First Evidence of the Role of Zonal Flows for the $L$ - $H$ Transition at Marginal Input Power in the EAST Tokamak

G. S. Xu,<sup>1</sup> B. N. Wan,<sup>1</sup> H. Q. Wang,<sup>1</sup> H. Y. Guo,<sup>1,2</sup> H. L. Zhao,<sup>3</sup> A. D. Liu,<sup>3</sup> V. Naulin,<sup>4</sup> P. H. Diamond,<sup>5</sup> G. R. Tynan,<sup>5</sup> M. Xu,<sup>5</sup> R. Chen,<sup>1</sup> M. Jiang,<sup>1</sup> P. Liu,<sup>1</sup> N. Yan,<sup>1</sup> W. Zhang,<sup>1</sup> L. Wang,<sup>1</sup> S. C. Liu,<sup>1</sup> and S. Y. Ding<sup>1</sup>

<sup>1</sup>*Institute of Plasma Physics, Chinese Academy of Sciences, Hefei 230031, China*

<sup>2</sup>*Tri Alpha Energy, Inc., P.O. Box 7010, Rancho Santa Margarita, California 92688, USA*

<sup>3</sup>*Department of Modern Physics, University of Science and Technology of China, Hefei 230026, China*

<sup>4</sup>*Association Euratom-Risø DTU, DK-4000 Roskilde, Denmark*

<sup>5</sup>*University of California, San Diego, 9500 Gilman Drive, La Jolla, California 92093, USA*

(Received 19 May 2011; published 14 September 2011)

A quasiperiodic  $E_r$  oscillation at a frequency of  $<4$  kHz, much lower than the geodesic-acoustic-mode frequency, with a modulation in edge turbulence preceding and following the low-to-high ( $L$ - $H$ ) confinement mode transition, has been observed for the first time in the EAST tokamak, using two toroidally separated reciprocating probes. Just prior to the  $L$ - $H$  transition, the  $E_r$  oscillation often evolves into intermittent negative  $E_r$  spikes. The low-frequency  $E_r$  oscillation, as well as the  $E_r$  spikes, is strongly correlated with the turbulence-driven Reynolds stress, thus providing first evidence of the role of the zonal flows in the  $L$ - $H$  transition at marginal input power. These new findings not only shed light on the underlying physics mechanism for the  $L$ - $H$  transition, but also have significant implications for ITER operations close to the  $L$ - $H$  transition threshold power.

DOI: 10.1103/PhysRevLett.107.125001

PACS numbers: 52.55.Fa, 52.25.Fi, 52.35.Ra

The high-confinement mode ( $H$  mode) is the projected baseline operational scenario for the International Tokamak Experimental Reactor (ITER) [1]. Predictions for the  $H$ -mode power threshold in ITER remain uncertain since the physics of the  $L$ - $H$  (low-to-high confinement mode) transition is not yet fully understood [2]. The earliest theories attributed the transition to an increase in the edge negative radial electric field ( $E_r$ ), i.e., the so-called “mean  $\mathbf{E} \times \mathbf{B}$  flows” [3] and a subsequent reduction in the level of edge turbulence. However, these models failed to account for the fast time scale associated with the transition. The most recent theories reveal the crucial role of time-varying  $E_r$ , i.e., so-called “zonal flows,” in triggering the transition by reducing the power threshold [4,5]. When the zonal flows were incorporated in an  $L$ - $H$  transition model [5], a limit-cycle oscillation forms at marginal input power due to a predator-prey-type competition between turbulence and zonal flows. This model predicted that the turbulent fluctuation level will be modulated by a low-frequency  $E_r$  oscillation, which is self-generated by turbulence-driven Reynolds stress close to the  $L$ - $H$  transition. Recently,  $\sim 3$  kHz quiet periods were detected by gas puff imaging (GPI), at least 30 ms before the transition, in  $L$ -mode edge plasmas of the NSTX spherical tokamak [6]. More recently a low-frequency oscillation was observed at low density before the  $L$ - $H$  transition in the ASDEX-U tokamak using Doppler reflectometry, which was attributed to the geodesic acoustic mode (GAM) [7]. Similar pulsing or “dithering” transitions were also preliminarily investigated in the DIII-D tokamak using Doppler reflectometry and beam emission spectroscopy

(BES) [8]. Similar oscillations also appear in the TJ-II stellarator [9]. However, no direct measurements of  $E_r$  and turbulent Reynolds stress are available in the previous work. This Letter reports the first observation of a quasiperiodic  $E_r$  oscillation preceding and following the  $L$ - $H$  transition at a much lower frequency than the GAM, but similar to the limit-cycle oscillation predicted by the model [5], and demonstrates the strong correlation of this  $E_r$  oscillation with the turbulent Reynolds stress.

The  $H$  mode has recently been achieved, for the first time, in the EAST tokamak ( $R_0 = 1.88$  m,  $a = 0.45$  m,  $B_t = 1.4$ – $2$  T,  $I_p = 0.4$ – $0.8$  MA) [10] by lower hybrid wave (LHW) current drive with total heating power limited to about 1 MW, which allows direct probing of the radial electric field and zonal flows inside the separatrix during the  $L$ - $H$  transition using an array of specifically designed fast moving Langmuir probes. To do this, two reciprocating Langmuir probes mounted at the outer midplane, toroidally separated by  $89^\circ$ , [11] were used to provide direct measurements of  $E_r$ , turbulent fluctuations and turbulent Reynolds stress at the plasma edge with 5 MHz sampling rate. The measurements were conducted using a probe array with two tips (measuring floating potentials  $\Phi_{f2}$  and  $\Phi_{f3}$ ) poloidally separated by  $\delta p = 8$  mm and a third tip (measuring floating potential  $\Phi_{f1}$ ) in the middle of them, radially sticking out by  $\delta r = 5$  mm [12]. The  $E_r$  was calculated as  $[\Phi_{f1} - (\Phi_{f2} + \Phi_{f3})/2]/\delta r$  and the Reynolds stress was estimated as  $\langle \tilde{v}_r \tilde{v}_p \rangle = \langle \tilde{E}_r \tilde{E}_p \rangle / B^2$ , where  $E_p = (\Phi_{f2} - \Phi_{f3})/\delta p$  and the tilde represents fluctuation components ( $> 10$  kHz). The toroidal mode number of the  $E_r$  oscillations reported in this Letter was

$n \sim 0$  or  $4, \dots$ , determined by the long-distance correlation technique [13].

Figure 1 shows a typical  $H$ -mode discharge achieved by LHW with loss power (the power flowing out of the core plasma through the separatrix)  $P_{\text{loss}} \sim P_{\text{th}}^{L-H} \sim 1.1$  MW, under the unbalanced double null divertor configuration with the ion  $\nabla B$  drift toward the major  $X$  point at the bottom. Here, the loss power  $P_{\text{loss}}$  and the threshold power  $P_{\text{th}}^{L-H}$  for transition from  $L$  to  $H$  mode are defined as in [14]. As shown in the figure, quasiperiodic oscillations at a frequency of  $<4$  kHz, preceding the main transition, appear on a number of diagnostics located near the lower divertor, including ion saturation current from divertor target embedded Langmuir probes [Fig. 1(b)], extreme ultraviolet (XUV) radiation [Fig. 1(c)], carbon III emission [Fig. 1(d)], and  $D\alpha$  emission [Fig. 1(e)]. These measurements indicate that the particle and heat fluxes towards the lower divertor [via the scrap-off layer (SOL) transport] are modulated at a low frequency, i.e.,  $<4$  kHz. The oscillations are coherent, as shown in the zoom-in plot in Fig. 1(f), and well correlated between these signals, but uncorrelated or sometimes weakly correlated with the Mirnov (MHD) signals on the high field side, indicating that these oscillations are mainly electrostatic in nature. The oscillation amplitude (RMS/MEAN) is rather small, typically only of  $\sim 3\%$  in target  $D\alpha$  signals, which is much smaller than that during “dithering” transitions [2]. In addition, the periods are also much shorter than the

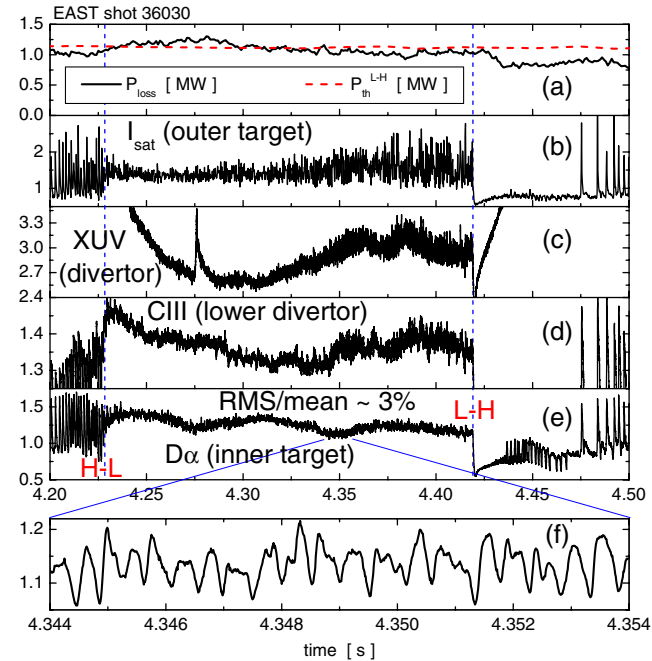


FIG. 1 (color online). (a) The loss power  $P_{\text{loss}}$  and the  $H$ -mode threshold power  $P_{\text{th}}^{L-H}$ , (b) the probe ion saturation on the outer target plate, (c) the XUV radiation from the divertor, (d) the carbon III emission from the divertor, (e) the  $D\alpha$  emission near the inner target, (f) 10 ms zoom-in plot of the  $D\alpha$  signal.

dithering periods. The oscillation amplitude usually slowly increases when approaching the transition, on  $\sim 100$  ms time scale, as shown in Fig. 1, but without a systematic increase within the last 10 ms prior to the transition.

These oscillations appear to originate from the plasma edge, and are not seen by core plasma diagnostics. To further investigate this, the probes were inserted into the edge plasma in the same discharge as shown in Fig. 1 at  $\sim 60$  ms before the transition. Figure 2(a) plots the raw signal of the floating potential  $\Phi_{f1}$  over 4 ms, showing a quasiperiodic modulation of fluctuations at a frequency of 2 kHz. During this period of time, the probe was inserted at  $\sim 1.5$  cm inside the separatrix. The Er and  $\Phi_{f1}$  fluctuation envelopes, as well as the divertor  $D\alpha$  emission, appear to oscillate at the same frequency and are well correlated. The envelope of fluctuations ( $> 10$  kHz) was calculated using the Hilbert transform technique [13]. The Reynolds stress also appears to be modulated at the same frequency, as shown in Fig. 2(e). The statistical errors in the Reynolds stress are about  $\pm 40\%$  based on the error analysis method described in [15]. In addition, the energy transfer rate between turbulence and fluctuating Er has been estimated using the measured Reynolds stress following the analysis in [15,16], i.e.,  $\gamma \equiv \langle v_p \rangle \langle \tilde{v}_r \tilde{v}_p \rangle / (\Delta r \langle \tilde{v}_p^2 \rangle)$ . The Reynolds stress is nearly zero in the SOL and increases radially inward, reaching  $\sim 1 \times 10^5$  m<sup>2</sup>/s<sup>2</sup> at  $\sim 1$  cm inside the separatrix, with radial gradient length  $\Delta r \sim 1$  cm. The

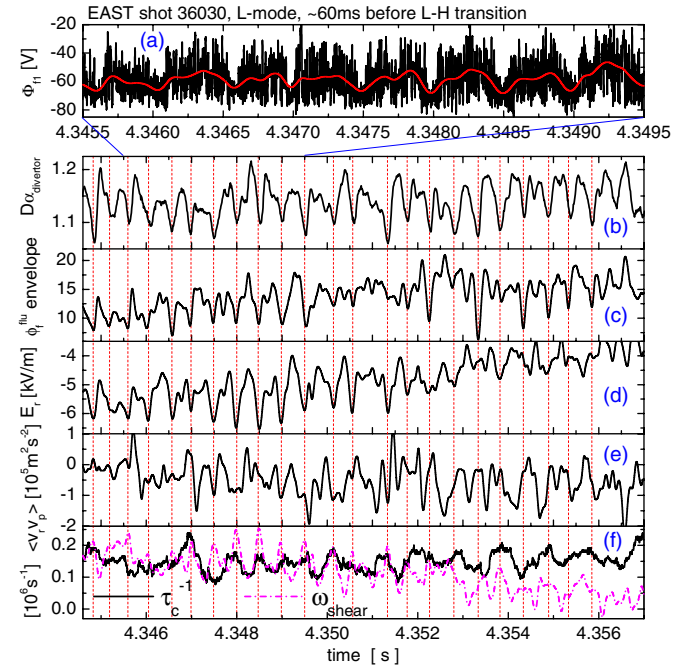


FIG. 2 (color online). (a) 4 ms raw data of the floating potential  $\Phi_{f1}$  and its low-frequency component,  $<5$  kHz, (b) the  $D\alpha$  emission near the inner target, (c) the  $\Phi_{f1}$  fluctuation envelope, (d) the radial electric field, (e) the turbulent Reynolds stress, (f) the turbulence decorrelation rate  $\tau_c^{-1}$  and the local Er shear rate  $\omega_{\text{shear}}$ .

poloidal velocity  $\langle v_p \rangle$  is  $\sim 2$  km/s and the fluctuating flow energy  $\langle \tilde{v}_p^2 \rangle$  is  $\sim 1 \times 10^6$  m<sup>2</sup>/s<sup>2</sup>. Hence, the calculated energy transfer rate  $\gamma$  is  $\sim 2 \times 10^4$  s<sup>-1</sup>. The zonal-flow damping rate at the plasma edge is of the order of the ion transit frequency  $v_{thi}/qR_0$  or the ion-ion collision frequency  $\tau_{ii}^{-1}$ , which are both of the order of  $1 \times 10^4$  s<sup>-1</sup> at the plasma edge [17], comparable with the calculated energy transfer rate. This indicates that the turbulence force is strong enough to overcome the damping force, thus driving the fluctuating Er.

Figure 2(f) compares the turbulence decorrelation rate  $\tau_c^{-1}$  and the local Er shearing rate  $\omega_{shear}$ .  $\tau_c^{-1}$  was estimated using the  $\Phi_{f1}$  fluctuation ( $> 10$  kHz).  $\omega_{shear}$  was estimated from the radial gradient of Er; i.e.,  $\omega_{shear} = (Er_1^* - Er_2^*) / (B\Delta r)$ , where  $Er_1^*$  and  $Er_2^*$  were simultaneously measured by two reciprocating probe arrays at two different radial locations with a radial separation  $\Delta r \sim 1$  cm. Here, an approximate correction due to the radial electron temperature gradient has been made with  $Er^* = Er - 2.8 \nabla Te$  [11], with the Te profile being obtained from a triple probe array in a similar discharge. The uncertainty in the shearing rate estimation is about  $\pm 30\%$ . Such estimated  $\tau_c^{-1}$  and  $\omega_{shear}$  rates are comparable, thus suggesting the Er modulation resulting from the interplay between turbulence drive and flow shear. As can be seen from Figs. 2(f) and 2(c), the fluctuations are significantly suppressed during the quiet periods, as  $\omega_{shear}$  temporally exceeds  $\tau_c^{-1}$ .

Figure 3(a) clearly shows a peak in the normalized floating potential fluctuation power spectra at 2 kHz with two harmonics at  $\sim 4$  and  $\sim 6$  kHz, and with the background turbulence peaking at  $\sim 80$  kHz. It is to be noted that on EAST, GAM oscillations usually appear at low plasma densities and high safety factors  $q$  with the typical frequency of 10–20 kHz. The  $H$ -mode discharges were typically achieved on EAST with central line average density  $> 1.8 \times 10^{19}$  m<sup>-3</sup> and low  $q$  (3–4), without coherent oscillations at 10–20 kHz being observed by the probes. Therefore, the GAM does not appear to be active in the  $L$ - $H$  transition process under these conditions. The normalized power spectra of the Er and  $\Phi_{f1}$  fluctuation envelopes and the divertor  $D\alpha$  emission also show a sharp coherent peak at 2 kHz, Fig. 3(b). Figure 3(c) plots the integrated wavelet bicoherence spectrum obtained from a wavelet bicoherence analysis using a complex Gaussian wavelet [18]. Clearly, the signals are well above the noise level in two frequency ranges, which demonstrates the existence of three-wave coupling between the turbulence in 30–100 kHz and the 2 kHz oscillation (and its harmonics). Figure 3(d) shows the cross-correlation function between  $|Er|$  and  $\Phi_{f1}$  fluctuation envelopes, which exhibits a negative peak at zero time delay, indicating an  $\sim 70\%$  correlation, i.e., nearly  $180^\circ$  out of phase. The cross-correlation function also exhibits a negative peak at zero time delay between  $\omega_{shear}$  and  $\tau_c$ , as shown in Fig. 3(f). It

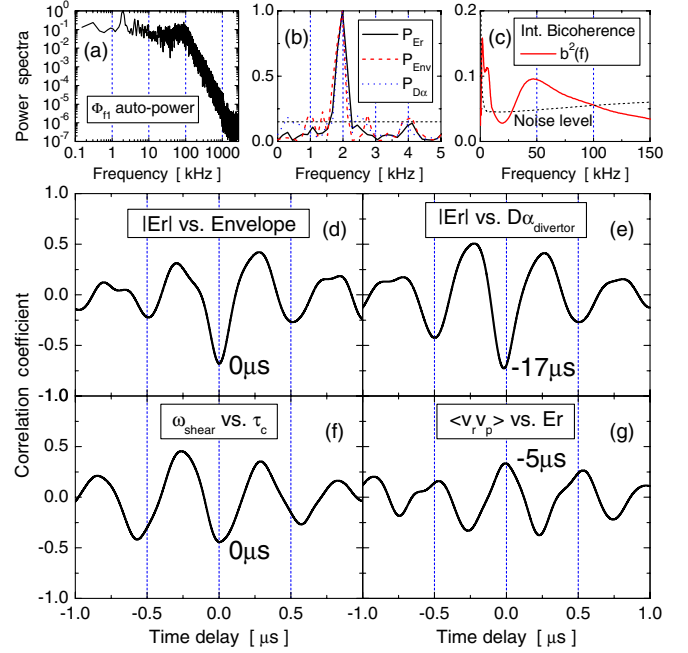


FIG. 3 (color online). (a) The normalized power spectrum of  $\Phi_{f1}$ , (b) the normalized power spectra of Er,  $\Phi_{f1}$  fluctuation envelope and divertor  $D\alpha$  emission, (c) the integrated wavelet bicoherence spectrum of  $\Phi_{f1}$ , the dashed curve shows the noise level. The cross-correlation functions between (d)  $|Er|$  and  $\Phi_{f1}$  fluctuation envelope, (e)  $|Er|$  and divertor  $D\alpha$  emission, (f) local Er shearing rate  $\omega_{shear}$  and the decorrelation time  $\tau_c$ , (g) turbulent Reynolds stress and Er.

is evident that the fluctuations are suppressed and decorrelated when the Er becomes more negative. Note also that the Er oscillation precedes the divertor  $D\alpha$  oscillation, as indicated by a  $17\text{-}\mu\text{s}$  negative time delay between  $|Er|$  and divertor  $D\alpha$  emission, thus implying the causality between them. Since the particle flux entering the SOL from the core plasma is controlled by the shear flow at the plasma edge, an oscillation in the edge Er shear could in principle modulate the SOL transport and hence the divertor  $D\alpha$  emission from recycling neutrals. The cross-correlation coefficient between Reynolds stress and Er is  $\sim 30\%$ , i.e., nearly in phase [Fig. 3(g)]. The existence of finite correlation and the short time delay between them are consistent with the theory that the zonal flows are driven by the turbulent Reynolds stress [4].

Here it is interesting to note that sawtooth heat pulses appear to affect or modulate these oscillations, and sometimes promote the  $L$ - $H$  transition. More detailed measurements will be made to further investigate this effect.

It needs to be clarified that quasiperiodic oscillations are not always present prior to the transition; the frequency of the Er oscillation may change with time and sometimes the frequency spectrum of the Er exhibits more broadband (still in the low-frequency range of  $< 4$  kHz) and intermittent features, e.g., as observed in DIII-D [19], ASDEX-U [20], HL-2A [13], and NSTX [21]. In the discharge shown

in Fig. 4, the probes captured an  $L$ - $H$  transition at 4.263 s, with the probe tip measuring the floating potential  $\Phi_{f1}$  located  $\sim 5$  mm inside the separatrix and the other two tips still near the separatrix. Just prior to the transition the Er oscillation evolves into several intermittent negative spikes, as shown in the zoom-in plot in Fig. 4(i). These Er spikes are well correlated with the Reynolds stress, as shown in Fig. 4(j), and exhibit a similar frequency to the quasiperiodic oscillations, thus indicating the same nature of turbulence regulation by zonal flows. They are also correlated with small bumps in the divertor  $D\alpha$  emission.

The Er oscillations were observed not only before but also after the transition in EAST. The oscillations usually disappear right after the transition, but slowly grow up again, along with a recovery in the edge turbulence level, presumably due to the steepening of the edge pressure gradient, as shown in Fig. 4. In this case, the  $H$  mode starts with a short edge-localized mode (ELM)-free period of  $\sim 50$  ms, followed by an ELMy- $H$  period. The onset of the divertor  $D\alpha$  oscillation appears at  $\sim 4.27$  s, Fig. 4(a), which then slowly grows up, with frequency gradually decreasing from  $\sim 4$  to below 1 kHz, coincident with a reduction in the ion-ion collision rate  $\tau_{ii}^{-1}$ , as shown in

Fig. 4(b). Since the zonal-flow damping is induced mainly by the ion-ion collision, the model [5] predicted that the frequency of the limit-cycle oscillation is controlled by  $\tau_{ii}^{-1}$ , consistent with the observation. The edge pressure gradient rises simultaneously, as evidenced by the increase in XUV radiation at  $r/a = 0.9$  [Fig. 4(c)]. As can be seen from Fig. 4(d), the floating potential  $\Phi_{f1}$  exhibits an abrupt reduction in the fluctuation level at the transition. Shortly after the transition the turbulence level recovers and the mean negative Er starts to increase, as shown in Fig. 4(g), possibly due to the steepening of the edge pressure gradient, which is generally regarded as the free energy source of the turbulence and the dominant drive of the mean Er according to neoclassical theories [3]. However, no significant change in the mean Er appears preceding the transition at the radial location for these particular measurements. Note that similar to the observations shown in Fig. 2(a), the fluctuation levels of  $\Phi_{f1}$  are modulated [Fig. 4(f)], and the Er,  $\Phi_{f1}$  fluctuation amplitudes and  $D\alpha$  emission [Fig. 4(e)] are strongly correlated. Hence, this demonstrates that the fluctuations and the SOL transport are modulated by the edge Er oscillations. Again, by carefully tracking the time series one can see that the  $D\alpha$

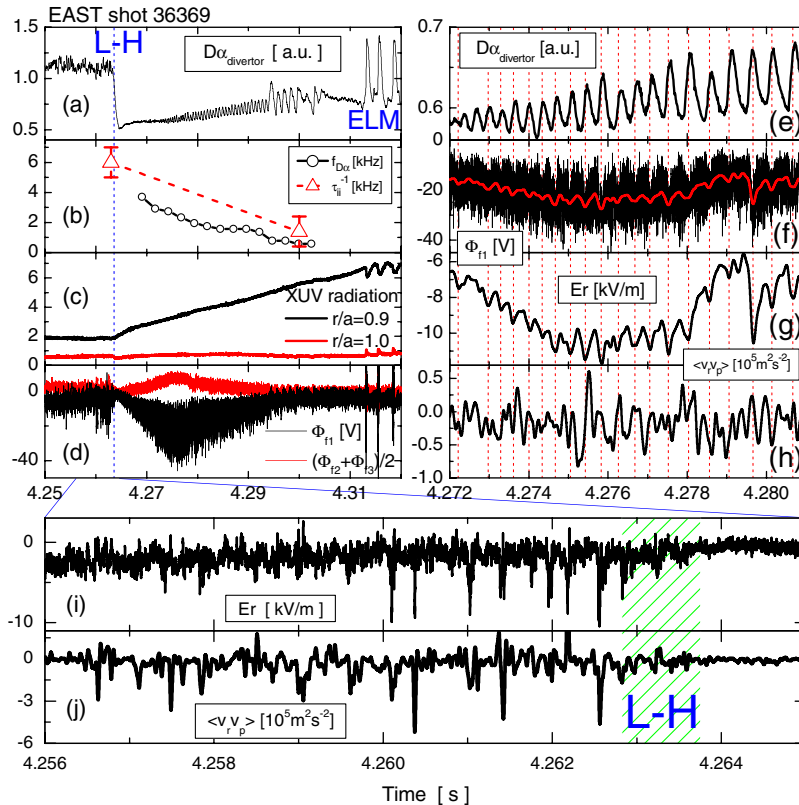


FIG. 4 (color online). (a) The divertor  $D\alpha$  emission signal, (b) the frequency of the oscillation in the  $D\alpha$  signal and the edge ion-ion collision rate  $\tau_{ii}^{-1}$ , (c) the XUV radiation signals at  $r/a = 0.9$  and  $1.0$ , (d) the floating potential signals  $\Phi_{f1}$  and  $(\Phi_{f2} + \Phi_{f3})/2$  measured by probes, (e) the same  $D\alpha$  signal as in (a) on an expanded time scale, (f) the floating potential  $\Phi_{f1}$  and its low-frequency component,  $<5$  kHz, (g) the radial electric field, (h) the turbulent Reynolds stress. The zoom-in plots of (i) the radial electric field and (j) the turbulent Reynolds stress near the transition.



oscillations lag behind the  $E_r$  oscillations, and that the Reynolds stress is also modulated at the same frequency as and well correlated with the  $E_r$  oscillation, as shown in Fig. 4(h). GAMs cannot be observed in the  $H$ -mode period in EAST, as in DIII-D [19] and ASDEX-U [7].

In summary, a quasiperiodic low-frequency  $E_r$  oscillation and a modulation in edge turbulence preceding and following the  $L$ - $H$  transition have been observed, for the first time, in EAST at marginal input power by direct probing inside the separatrix. Wavelet bicoherence analysis shows a strong coupling between edge turbulence and the low-frequency  $E_r$  oscillations below 4 kHz, and the turbulence Reynolds stress is well correlated with the  $E_r$  oscillation. The frequency of the  $E_r$  oscillation is much lower than the expected GAM frequency (no coherent oscillations in the GAM frequency range can be detected by the probes in these experiments), but similar to that of limit-cycle oscillations predicted by a more recent  $L$ - $H$  transition model [5], which takes into account the contribution from zonal flows. Just prior to the transition the  $E_r$  oscillation often evolves into intermittent negative  $E_r$  spikes. The  $E_r$  oscillation reappears following the transition and slowly grows, but with a gradual reduction in frequency, along with a recovery in the edge turbulence level and an increase in the mean negative  $E_r$ , possibly due to the steepening of the edge pressure gradients.

This work was supported by the National Natural Science Foundation of China under Contracts No. 11075181, No. 10725523, No. 10721505, No. 10990212, No. 10605028, the National Magnetic Confinement Fusion Science Program of China under Contracts No. 2010GB104001 and No. 2011GB107001, the CAS pilot project of emerging and interdisciplinary

subjects, and the Sino Danish Center for Education and Research. We gratefully acknowledge the contribution of the EAST staff.

- 
- [1] C. Gormezano *et al.*, *Nucl. Fusion* **47**, S285 (2007).
  - [2] F. Wagner, *Plasma Phys. Controlled Fusion* **49**, B1 (2007).
  - [3] H. Biglari, P. H. Diamond, and P. W. Terry, *Phys. Fluids B* **2**, 1 (1990).
  - [4] P. H. Diamond *et al.*, *Phys. Rev. Lett.* **72**, 2565 (1994).
  - [5] E. J. Kim and P. H. Diamond, *Phys. Rev. Lett.* **90**, 185006 (2003).
  - [6] S. J. Zweben *et al.*, *Phys. Plasmas* **17**, 102502 (2010).
  - [7] G. D. Conway *et al.*, *Phys. Rev. Lett.* **106**, 065001 (2011).
  - [8] L. Schmitz and Z. Yan, Joint US-EU Transport Task Force Meeting (San Diego, 2011) [<http://tff2011.pppl.gov/>].
  - [9] T. Estrada *et al.*, *Europhys. Lett.* **92**, 35001 (2010).
  - [10] G. S. Xu *et al.*, *Nucl. Fusion* **51**, 072001 (2011).
  - [11] W. Zhang *et al.*, *Rev. Sci. Instrum.* **81**, 113501 (2010).
  - [12] G. S. Xu *et al.*, *Phys. Rev. Lett.* **91**, 125001 (2003).
  - [13] A. D. Liu *et al.*, *Phys. Rev. Lett.* **103**, 095002 (2009).
  - [14] Y. R. Martin and T. Takizuka, *J. Phys. Conf. Ser.* **123**, 012033 (2008).
  - [15] E. Sánchez *et al.*, *J. Nucl. Mater.* **337–339**, 296 (2005).
  - [16] G. S. Xu *et al.*, *Nucl. Fusion* **49**, 092002 (2009).
  - [17] P. H. Diamond *et al.*, *Plasma Phys. Controlled Fusion* **47**, R35 (2005).
  - [18] B. Ph. van Milligen *et al.*, *Phys. Plasmas* **2**, 3017 (1995).
  - [19] G. R. McKee *et al.*, *Nucl. Fusion* **49**, 115016 (2009).
  - [20] G. D. Conway *et al.*, *Plasma Phys. Controlled Fusion* **47**, 1165 (2005).
  - [21] Y. Sechrest *et al.*, *Phys. Plasmas* **18**, 012502 (2011).